



VICTORIA UNIVERSITY
MELBOURNE AUSTRALIA

Using machine learning to examine associations between the built environment and physical function: A feasibility study

This is the Accepted version of the following publication

Rachele, Jerome, Wang, Jingcheng, Wijnands, Jasper S, Zhao, Haifeng, Bentley, Rebecca and Stevenson, Mark (2021) Using machine learning to examine associations between the built environment and physical function: A feasibility study. *Health and Place*, 70. ISSN 1353-8292

The publisher's official version can be found at
<https://www.sciencedirect.com/science/article/abs/pii/S1353829221000976>
Note that access to this version may require subscription.

Downloaded from VU Research Repository <https://vuir.vu.edu.au/42432/>

Using machine learning to examine associations between the built environment and physical function: A feasibility study

Abstract

Linking geospatial neighbourhood design characteristics to health and behavioural data from population-representative cohorts is limited by data availability and difficulty collecting information on environmental characteristics (e.g. greenery, building setbacks, dwelling structure). As an alternative, this study examined the feasibility of Generative Adversarial Networks (GANs) – machine learning – to measure neighbourhood design using ‘street view’ and aerial imagery to explore the relationship between the built environment and physical function. This study included 3101 adults aged 45 years and older clustered in 200 neighbourhoods in 2016 from the How Areas in Brisbane Influence Health and Activity (HABITAT) project in Brisbane, Australia. Exposure data were Google Street View and Google Maps images from within the 200 neighbourhoods, and outcome data were self-reported physical function using the PF-10 (a subset of the SF-36). Physical function scores were aggregated to the neighbourhood level, and the highest and lowest 20 neighbourhoods respectively were used in analysis. We found that the aerial imagery retrieved was unable to be used to adequately train the model, meaning that aerial imagery failed to produce meaningful results. Of the street view images, n=56,330 images were downloaded and used to train the GAN model. Model outputs included augmented street view images between neighbourhoods classed as having high function and low function residents. The GAN model detected differences in neighbourhood design characteristics between neighbourhoods classed as high and low physical function at the aggregate level, specifically differences were identified in urban greenery (including tree heights) and dwelling structure (e.g. building height). This study provides important lessons for future work in this field, especially related to the uniqueness, diversity and amount of imagery required for successful applications of deep learning methods.

Keywords: built environment; machine learning; physical function; feasibility study

Background

An individual's physical function declines with age, with the trajectory of this decline determining the age at which individuals are likely to lose independence in undertaking activities of daily living (1). The rate at which an individual's function declines is strongly influenced by a variety of modifiable individual-level lifestyle factors such as physical activity (2), smoking, diet, and alcohol consumption (3), as well as environmental-level factors: the characteristics of the places in which people live. These environmental-level factors, hereafter referred to as the built environment, are typically defined as a set of objective and perceived characteristics of the physical context in which people live, and include aspects of urban design, availability of local destinations (e.g. stores, public transit), traffic volume and speed, and distance to and design of venues for physical activity (e.g., parks) (4). It has been postulated that these built environment characteristics influence individual-level health behaviours, and consequentially the rate of decline of physical function, through the provision of a setting for health-enhancing behaviours to occur (5).

Typical epidemiological approaches to understanding how the built environment is associated with health behaviours and outcomes is through examining associations between the built environment characteristics, measured either using geographical information system (GIS) data (6) linked to behavioural data from population-representative cohorts, self-reported data on the local built environment from participants themselves, or environmental audits (7). Of 23 quantitative studies examining associations between the built environment and physical function in a recent systematic review (8), 10 studies (9-18) used self-report measures and 13 (19-31) used objective measures (e.g., GIS-based measures, census data or similar). Studies assessed features related to the participants' home including the home external appearance and building setbacks (16, 20, 26), in-home interviews to assess features around the home (23), a combination of community mobility barriers and transportation facilities (11, 17), while several measured some form of 'neighbourhood problems' or signs of physical disorder such as litter, graffiti or vandalism (9, 12-15, 21). However, common approaches of measuring built environment

characteristics are often limited by only being able to include a single, or very few, built environment characteristics, or by the availability of data.

Open-source, publicly available data sources are increasingly being used as a method of measuring built environment characteristics (32). For example, Google Street View, Google maps, and Google satellite imagery provide information from different perspectives. Street view images offer street-level panoramic photography and incorporate detailed information of the objects in the streetscape. Map images are more abstract, semantically rich images, and provide not only locations and boundaries of visible objects such as roads, parks, buildings, rivers and facilities, but also additional information such as public transport routes and terrain. As a big data source covering half the world's population and up to ten years historical data, Google Street View images have substantial research advantages (33, 34). Google maps, including satellite imagery, can be downloaded using the Google Maps API, allowing custom settings of locations, map types, and zoom levels.

Approaches to analyse these increasingly large datasets, including machine learning methods, have attracted substantial interest within the scientific community. Machine learning is a sub-field of artificial intelligence, focussing on training computers to perform specific tasks (e.g., classification, prediction) using large datasets. Machine learning algorithms developed for these purposes include support vector machines, decision trees and graphical models. These algorithms have been used successfully for a wide variety of tasks such as spam filtering (35), land cover classification (36), fraud detection (37) and weather forecasting (38). A specific field of machine learning, deep learning, has achieved major advances in performance by radically increasing both the number of parameters in the model and the amount of data used to train them (39). Using deep learning, computers have now reached super-human performance in tasks ranging from playing board games (40) to image classification (41). So, how can machine learning be combined with satellite and street-view images to measure the built environment, and how does it differ from existing approaches like GIS or in-person or desktop audits? First, geospatial data can be difficult to obtain, and in some cases is inaccurate, incomplete, or simply not collected and

therefore does not exist (42). And second, approaches to analysing existing street view (in-person and desktop) data have typically used audits (e.g. POSDAT (43)). However, these are often time-consuming, labour-intensive, expensive exercises. Machine learning methods dramatically increase the feasibility of using satellite and street view imagery for measurement of the built environment. Even using unsupervised machine learning approaches such as autoencoders (44), models are able to identify key environmental characteristics including vegetation, building size and design, road design, and transit stops (45). Autoencoders achieve this by using the image itself as the output label, while passing the data through a narrow bottleneck layer for feature extraction.

In this study, we investigate the concept of image style transfer, where deep learning is used to merge the content of one image with the style of a different image (e.g., (46, 47)). This concept can be extended to understand associations between the built environment and health by defining facilities and the urban layout, e.g., streets/building patterns (urban morphology) as content, and health outcomes as style (48). Translating an urban area to different styles, for example, from low health to good health, facilitates goal-oriented outcome transformation: by comparing the changes between the urban design characteristics before and after style transfer, we can gain an understanding of how neighbourhood characteristics might be associated with health. The advantage of this method is that it is not targeting a few selected factors, instead it explores all potential factors captured in the selected imagery at once. As the method is purely based on objective imagery information, it eliminates the possible bias caused by people in traditional human participated research methods. Beyond the application of exploring the health inequalities, this method can be readily extended to more broader applications, as maps of different types are available such as maps for terrain, land use, and public transport.

Aim

This study aims to use generative adversarial networks (GANs) to understand the association between built environment characteristics and physical function. This will be achieved through combining residential geo-codes and health outcomes from a population representative study of the social

determinants of health with imagery from Google Maps and Google Street View. Model outputs will be GAN-generated examples of neighbourhood design and streetscape characteristics associated with inequalities in physical function.

Methods

GANs are an unsupervised machine learning technique for realistic image generation. Based on imagery from two domains of interest, the UNsupervised Image-to-image Translation (UNIT) framework (49) uses a pair of GANs to achieve domain translation based on the assumption of the existence of a shared latent space, encoding common features. The open-sourced UNIT framework is used in this study for both training and translation purpose.

The HABITAT Study

This study used data from the How Areas in Brisbane Influence health And acTivity (HABITAT) project (50). HABITAT is a multilevel longitudinal (2007-2018) study of mid-aged adults (40 – 65 years in 2007) living in Brisbane, Australia. The primary aim of HABITAT is to examine patterns of change in physical activity, sedentary behaviour and health over the period 2007 – 2018 and to assess the relative contributions of environmental, social, psychological and socio-demographic factors to these changes. Details about HABITAT's sampling design have been published elsewhere (50). Briefly, a multi-stage probability sampling design was used to select a stratified random sample (n=200) of Census Collector's Districts (CCD) (from a total of n=1625) from the Australian Bureau of Statistics, and from within each CCD, a random sample of people aged 40–65 years (n=16,127).

Physical function

This was measured using the Physical Function Scale (PF-10), a component of the Short Form 36 Health Survey (51). The stem question of the PF-10 asked 'Does your health now limit you in these activities? If

so, how much?'. Respondents were given the following choices as response for each activity: 'Yes, limited a lot', 'Yes, limited a little' or 'No, not limited at all'. The PF-10 measures a hierarchical range of difficulties, from vigorous activities, such as lifting heavy objects to bathing and dressing (52). This measure has been extensively validated among community-dwelling adults using convergent validity calculated by Pearson correlations using three performance-based measures: single limb stance as an indicator of balance ($r = 0.42$), Time Up and Go test as a measure of mobility ($r = -0.70$) and gait speed as an indicator of overall functional capacity ($r = 0.75$) (53). The method of data cleaning for the physical function score was adapted from Ware, Kosinski (51). The raw physical function scores were calculated as the sum of re-coded scale items and were transformed to a 0 to 100 scale, where 0 represents minimal functioning, and 100 represents maximal functioning.

Identifying areas

In 2016, 3102 participants remained in the HABITAT study in their original area-level cluster (60.0% of Wave 5 respondents and 28.1% of the baseline sample). Initial plots of the data did not identify distinct clusters of participants that could be classified as either low or high physical function. Participants were therefore divided into two domains in order to maximise the chances of identifying differences in neighbourhood characteristics based on our outcome of interest: the highest and lowest 10% of physical function were kept in the analytic sample, leaving 618 participants divided evenly into 'high physical function' and 'low physical function' domains. Given that 618 images were insufficient for deep learning, rather than retrieving images at the coordinates of the 618 samples, these coordinates were used to form clusters using k -means to obtain neighbourhoods corresponding to high and low physical function. The k -means algorithm was selected to specify neighbourhoods as it allowed for the specification of the final number of clusters. This was considered more important than specifying the number of data points within each cluster, using alternate methods such as k -nearest neighbours. A plot of the coordinates of each of the 3102 participants is presented in Supplementary Material 1. Details of the analytic sample are presented in Table 1. For each of the clusters, the cluster centre was determined, and images were

retrieved around it. A bounding box was drawn around the centre, and the size of the bounding box was obtained by computing the average minimum distance (the distance from one cluster to its closest neighbour cluster) to ensure there was no overlap between the bounding boxes. Each bounding box had a size around 260 by 260m. All images were downloaded in March 2019 using the latest available images. While the majority of images were between 2013 and 2018, some images retrieved were from as early as 2009.

TABLE 1 ABOUT HERE

Aerial imagery retrieval

Aerial imagery was downloaded using Google Maps Static API, which allows users to customise parameters including the centre of the map, zoom level of the region, size of the image, and the type of map (54). Several map types are available including roadmap, satellite, hybrid, and terrain. The Maps Static API also allows users to define the style of maps including the colour, brightness and visibility of features (and their markers) such as roads, water, transit, landscape, points of interest and administrative areas. Aerial imagery has some advantages over street view images in that it is more structured. Different colours can be applied to different features, and unwanted features and their markers can be excluded. For example, Figure 1 contains a customised roadmap image (map type: road map, size: 256x256, zoom level: 19) with the background defined as white, roads as black, water as blue, and parks as green.

FIGURE 1 ABOUT HERE

Google street view image retrieval

For each bounding box, points were selected every 10 meters, and for each point, eight images were retrieved using different heading angles (0, 45, 90, 135, 180, 225, 270, 315). Images were not retrieved where data were not available on Google Street View, or where images were out of scope for this study

(e.g., in underground road tunnels). This led to the retrieval of 29,282 images for high physical function clusters and 27,048 images for low physical function clusters (56,330 in total). The model extracted particular characteristics of the built environment, such as vegetation, building size and design, and road design, implicitly, as these features are required to successfully reconstruct an image.

Analysis

Model training procedures

The UNIT framework was trained using (model settings and parameters available in Supplementary Material 2) on the general purpose GPU cluster of the University of Melbourne's high-performance computing infrastructure. Following model training, images from each domain were translated into their other respective domains, i.e., 'high functioning neighbourhood' to 'low functioning neighbourhood' and vice-versa.

We used the default hyperparameters from the UNIT framework, available in Supplementary Material 2. The weights in the deep learning model were calibrated using small batches of images, limited by available GPU memory (in this study, one batch contained four images). Batches were used to iteratively update parameters in both the generative model and the discriminator using a low learning rate, alternating between the two models. This resulted in the generative model creating images of progressively better quality, while the discriminator also improved in its ability to assess whether an image was generated or real. Hence, this game-theoretic approach allowed both models to improve. After model calibration, only the generative model is required to generate realistic images. Given that areas are identified based on participants' physical function, physical function in this scenario is considered the explanatory variable, while environment attributes would be considered the outcome variable – given that built environment characteristics are produced from the model. We programmed the model to provide 'snapshots' every 1000 iterations. The discriminator model within the GAN attempted to guide the

training in such a way that translated images looked realistic. For validation purposes, snapshots were sampled and evaluated visually as well every 1000 iterations. Terminating the training process after 5000 iterations (and 40,000 images passing through the model) was assessed to be optimal.

Results

Aerial imagery

The aerial imagery retrieved was unable to be used to adequately train the model. A combination of the nature of the aerial imagery retrieved being too similar, and an insufficient number of images able to be retrieved due to the clustered nature of the sample, meant that aerial imagery failed to produce meaningful results.

Street view imagery

Image translation from ‘high physical function’ to ‘low physical function’ neighbourhoods revealed two key changes: 1) the removal of vegetation, particularly in the upper portion of images; and 2) the removal of the upper floors of buildings. These findings are presented in Figure 2.

FIGURE 2 ABOUT HERE

Image translation from ‘low physical function’ to ‘high physical function’ neighbourhoods revealed only one key change, namely, the addition of vegetation. These findings are presented in Figure 3.

FIGURE 3 ABOUT HERE

Discussion

This study found associations between higher physical function and the greater amounts of vegetation and denser residential dwellings. The number of aerial images for each area defined as high and low physical

function was insufficient, even at high levels of zoom, to train deep learning models. Even for small neighbourhoods, increasing the number of aerial images in a cluster by downloading images with overlapping areas increased the quantity, but the quality of training was poor due to a lack of variation in these images. This study downloaded roadmap images and satellite images for each cluster using different zoom levels. The small zoom levels captured more information about the broader neighbourhood, while aerial imagery with larger zoom levels captured more local information of a neighbourhood; therefore, combining aerial imagery with different zoom levels depicted a neighbourhood from more aspects than aerial imagery with one single zoom level. In order to use aerial imagery successfully, a larger spatial spread of sampled domain locations is required. For example, a study examining street layout with method of travel to work using Census data may be a more feasible use of aerial imagery.

A recent systematic review of the association between the built environment and physical function found strong evidence for the importance of pedestrian infrastructure and aesthetics, while weaker evidence was found for land use mix, safety from crime and traffic, and an insufficient number of studies for walkability, residential density, street connectivity and access to public transport (8). While our study identified the importance of vegetation, the literature on green space is both limited and mixed. Of two previous studies that have examined the association between green space and physical function, one had a null association (28), while the other was positive (30). Further, while the current study did not identify any streetscape characteristics in image-to-image translation, several existing studies have identified positive associations between physical function and positive street characteristics (19), the presence of benches (18), positive front entrance features of dwellings (20) and unbroken footpaths (16). One possible explanation for this is that the study area, Brisbane, Australia, is controlled by one large local government area. This means that policies regarding streetscape infrastructure such as footpaths are likely to be similar between study areas if the same policies are applied everywhere. This is in contrast to a similar study undertaken examining the potential of Street View images and health (48) conducted in Melbourne, which has over 30 local government areas.

This study has several limitations. First, the descriptive, cross-sectional nature of the analysis meant that the study was limited in its ability to infer causation between urban design characteristics. Indeed, it is very plausible that people would select into low-set dwellings due to their poorer physical function. Second, some of the images downloaded, and also translated, were of poorer quality. However, these inaccuracies were unlikely to have influenced the findings of this study. Third, there were some inherent biases from use of the HABITAT study. Survey non-response in the HABITAT baseline study was 31.5%, and slightly higher among residents from lower individual socioeconomic profiles, and those living in more disadvantaged neighbourhoods. Further, this study used the fifth wave of HABITAT, which has experienced attrition over the life of the study. Like most longitudinal studies, this drop-out was more likely in the socioeconomically disadvantaged and those with poorer health. However, analyses have shown that HABITAT attrition is consistent with a Missing at Random pattern (55). Finally, the generalisability of this study's findings are likely to be limited to cities with similar built environments to Brisbane, Australia, including population distribution and the spatial patterning of built environment characteristics. Further information on the built environment can be found elsewhere (56). Briefly, Brisbane is characterised by relatively walkable inner city neighbourhoods with good access to large parks; however, there is limited public transport and walkable communities in the outer suburban areas.

There are several future research priorities. First, scope to identify causal relationships may become more feasible if temporal Street View data also becomes available and can be linked to available cohort studies. Examining associations between changes in built environments over time and changes in the trajectory of physical function decline would provide a much stronger basis to infer causation than in the current cross-sectional study design. Second, use of aerial imagery in future work would greatly complement the current study findings. Aerial imagery is able to capture broader urban design features important to physical function (e.g., the connectivity of street networks, and neighbourhood proportions of green and blue space) that are difficult to capture in street view imagery. Future research should endeavour to

replicate the methods of the current study with much larger sample sizes (e.g. census data) that can be linked to sufficient aerial imagery to train a GAN model.

Acknowledgements

This research was undertaken using the LIEF HPC-GPGPU Facility hosted at the University of Melbourne. This Facility was established with the assistance of LIEF Grant LE170100200. The HABITAT study is funded by the National Health and Medical Research Council (NHMRC) (ID 497236, 339718, 1047453). At the time that this paper was written, JNR was supported by the National Health and Medical Research Council (NHMRC) Centre for Research Excellence in Disability and Health (APP1116385), and an ARC Discovery Project (DP170101434). MS is supported by an NHMRC Fellowship (APP1136250).

References

1. World Health Organisation. Active Ageing: A Policy Framework. 2002.
2. Manini TM, Pahor M. Physical activity and maintaining physical function in older adults. *Brit J Sports Med.* 2009;43(1):28-31.
3. Hutchison T, Morrison P, Mikhailovich K. A review of the literature on active ageing. In: Health Impact Research Centre for Health Promotion and Wellbeing, editor. Canberra. 2006.
4. Cerin E, Nathan A, Van Cauwenberg J, Barnett DW, Barnett A. The neighbourhood physical environment and active travel in older adults: a systematic review and meta-analysis. *Int J Behav Nutr Phys Act.* 2017;14(1):15.
5. Papas MA, Alberg AJ, Ewing R, Helzlsouer KJ, Gary TL, Klassen AC. The built environment and obesity. *Epidemiologic Rev.* 2007;29(1):129-43.

6. Zhu X. GIS for environmental applications: a practical approach. Routledge; 2016.
7. Barnett DW, Barnett A, Nathan A, Van Cauwenberg J, Cerin E. Built environmental correlates of older adults' total physical activity and walking: a systematic review and meta-analysis. *Int J Behav Nutr Phys Act.* 2017;14(1):103.
8. Rachele JN, Sugiyama T, Davies S, Loh VHY, Turrell G, Carver A, et al. Neighbourhood built environment and physical function among mid-to-older aged adults: A systematic review. *Health & Place.* 2019;58:102137.
9. Balfour JL, Kaplan GA. Neighborhood environment and loss of physical function in older adults: evidence from the Alameda County Study. *Am J Epidemiol.* 2002;155(6):507-15.
10. Byles JE, Mackenzie L, Redman S, Parkinson L, Leigh L, Curryer C. Supporting housing and neighbourhoods for healthy ageing: Findings from the Housing and Independent Living Study (HAIL). *Australasian J Ageing.* 2014;33(1):29-35.
11. Keysor JJ, Jette AM, LaValley MP, Lewis CE, Torner JC, Nevitt MC, et al. Community environmental factors are associated with disability in older adults with functional limitations: the MOST study. *J Gerontol Series A.* 2010;65(4):393-9.
12. Latham K, Williams MM. Does neighborhood disorder predict recovery from mobility limitation? Findings from the Health and Retirement Study. *J Aging Health.* 2015.
13. Nguyen TT, Rist PM, Glymour MM. Are self-reported neighbourhood characteristics associated with onset of functional limitations in older adults with or without memory impairment? *J Epidemiol Community Health.* 2016.

14. Steptoe A, Feldman PJ. Neighborhood problems as sources of chronic stress: development of a measure of neighborhood problems, and associations with socioeconomic status and health. *Ann Behav Med.* 2001;23(3):177-85.
15. Walsh K, Gannon B. Perceived neighbourhood context, disability onset and old age. *J Socio-Economics.* 2011;40(5):631-6.
16. Werngren-Elgström M, Carlsson G, Iwarsson S. Changes in person-environmental fit and ADL dependence among older Swedish adults. A 10-year follow-up. *Aging Clin Exp Res.* 2008;20(5):469-78.
17. White DK, Jette AM, Felson DT, LaValley MP, Lewis CE, Torner JC, et al. Are features of the neighborhood environment associated with disability in older adults? *Disab Rehab.* 2010;32(8):639-45.
18. Sakari R, Rantakokko M, Portegijs E, Iwarsson S, Sipilä S, Viljanen A, et al. Do Associations Between Perceived Environmental and Individual Characteristics and Walking Limitations Depend on Lower Extremity Performance Level? *J Aging Health.* 2017;29(4):640-56.
19. Beard JR, Blaney S, Cerda M, Frye V, Lovasi GS, Ompad D, et al. Neighborhood characteristics and disability in older adults. *J Gerontol Series B.* 2009:gbn018.
20. Brown SC, Mason CA, Perrino T, Lombard JL, Martinez F, Plater-Zyberk E, et al. Built environment and physical functioning in Hispanic elders: the role of "eyes on the street". *Env Health Persp.* 2008;116(10):1300.
21. Clarke P, Ailshire JA, Bader M, Morenoff JD, House JS. Mobility disability and the urban built environment. *Am J Epidemiol.* 2008;168(5):506-13.
22. Clarke P, George LK. The role of the built environment in the disablement process. *Am J Public Health.* 2005;95(11):1933-9.

23. Clarke PJ. The role of the built environment and assistive devices for outdoor mobility in later life. *J Gerontol Series B*. 2014;69(Suppl 1):S8-S15.
24. Freedman VA, Grafova IB, Schoeni RF, Rogowski J. Neighborhoods and disability in later life. *Soc Sci Med*. 2008;66(11):2253-67.
25. Michael YL, Gold R, Perrin NA, Hillier TA. Built environment and lower extremity physical performance: prospective findings from the study of osteoporotic fractures in women. *J Aging Health*. 2011.
26. Schootman M, Andresen EM, Wolinsky FD, Malmstrom TK, Miller JP, Miller DK. Effect of street connectivity on incidence of lower-body functional limitations among middle-aged African Americans. *Ann Epidemiol*. 2012;22(8):568-74.
27. Takahashi PY, Baker MA, Cha S, Targonski PV. A cross-sectional survey of the relationship between walking, biking, and the built environment for adults aged over 70 years. *Risk Manag Health Policy*. 2012;5:35.
28. Vogt S, Mielck A, Berger U, Grill E, Peters A, Döring A, et al. Neighborhood and healthy aging in a German city: distances to green space and senior service centers and their associations with physical constitution, disability, and health-related quality of life. *Eur J Aging*. 2015;12(4):273-83.
29. Etman A, Kamphuis CB, Pierik FH, Burdorf A, Van Lenthe FJ. Residential area characteristics and disabilities among Dutch community-dwelling older adults. *Int J Health Geographics*. 2016;15(1):42.
30. Nascimento CFd, Duarte YAO, Lebrao ML, Chiavegatto Filho ADP. Individual and neighborhood factors associated with functional mobility and falls in elderly residents of São Paulo, Brazil: A multilevel analysis. *J Aging Health*. 2018;30(1):118-39.

31. Soma Y, Tsunoda K, Kitano N, Jindo T, Tsuji T, Saghadzadeh M, et al. Relationship between built environment attributes and physical function in Japanese community-dwelling older adults. *Geriatrics Gerontol Int.* 2017;17(3):382-90.
32. Rzotkiewicz A, Pearson AL, Dougherty BV, Shortridge A, Wilson N. Systematic review of the use of Google Street View in health research: major themes, strengths, weaknesses and possibilities for future research. *Health & place.* 2018;52:240-6.
33. Gebru T, Krause J, Wang Y, Chen D, Deng J, Aiden EL, et al. Using deep learning and google street view to estimate the demographic makeup of the us. arXiv preprint arXiv:170206683. 2017.
34. Kang J, Körner M, Wang Y, Taubenböck H, Zhu XX. Building instance classification using street view images. *ISPRS Journal of Photogrammetry and Remote Sensing.* 2018.
35. Amayri O, Bouguila N. A study of spam filtering using support vector machines. *Artificial Intelligence Review.* 2010;34(1):73-108.
36. Pal M, Mather PM. An assessment of the effectiveness of decision tree methods for land cover classification. *Remote sensing of environment.* 2003;86(4):554-65.
37. Perols J. Financial statement fraud detection: An analysis of statistical and machine learning algorithms. *Auditing: A Journal of Practice & Theory.* 2011;30(2):19-50.
38. Wijnands J, Qian G, Shelton K, Fawcett R, Chan J, Kuleshov Y. Seasonal forecasting of tropical cyclone activity in the Australian and the South Pacific Ocean regions. *Mathematics of Climate and Weather Forecasting.* 2015;1(1).
39. Schmidhuber J. Deep learning in neural networks: An overview. *Neural networks.* 2015;61:85-117.

40. Silver D, Huang A, Maddison CJ, Guez A, Sifre L, Van Den Driessche G, et al. Mastering the game of Go with deep neural networks and tree search. *nature*. 2016;529(7587):484.
41. He K, Zhang X, Ren S, Sun J, editors. Delving deep into rectifiers: Surpassing human-level performance on imagenet classification. *Proceedings of the IEEE international conference on computer vision*; 2015.
42. Stewart OT, Carlos HA, Lee C, Berke EM, Hurvitz PM, Li L, et al. Secondary GIS built environment data for health research: Guidance for data development. *Journal of transport & health*. 2016;3(4):529-39.
43. Edwards N, Hooper P, Trapp GS, Bull F, Boruff B, Giles-Corti B. Development of a public open space desktop auditing tool (POSDAT): a remote sensing approach. *Applied Geography*. 2013;38:22-30.
44. Ballard DH, editor *Modular learning in neural networks*. AAAI; 1987.
45. Mnih V, Hinton GE, editors. Learning to detect roads in high-resolution aerial images. *European Conference on Computer Vision*; 2010: Springer.
46. Gatys LA, Ecker AS, Bethge M, editors. Image style transfer using convolutional neural networks. *Proceedings of the IEEE conference on computer vision and pattern recognition*; 2016.
47. Zhang L, Ji Y, Lin X, Liu C, editors. Style transfer for anime sketches with enhanced residual u-net and auxiliary classifier gan. *2017 4th IAPR Asian Conference on Pattern Recognition (ACPR)*; 2017: IEEE.
48. Wijnands JS, Nice KA, Thompson J, Zhao H, Stevenson M. Streetscape augmentation using generative adversarial networks: insights related to health and wellbeing. *Sustainable Cities and Society*. 2019.

49. Liu M-Y, Breuel T, Kautz J, editors. Unsupervised image-to-image translation networks. *Advances in neural information processing systems*; 2017.
50. Burton NW, Haynes M, Wilson L-AM, Giles-Corti B, Oldenburg BF, Brown WJ, et al. HABITAT: A longitudinal multilevel study of physical activity change in mid-aged adults. *BMC Public Health*. 2009;9(1):76.
51. Ware JE, Kosinski M, Keller S. SF-36 physical and mental health summary scales: a user's manual: Health Assessment Lab.; 1994.
52. Haley SM, McHorney CA, Ware JE, Jr. Evaluation of the MOS SF-36 physical functioning scale (PF-10): I. Unidimensionality and reproducibility of the Rasch item scale. *Journal of Clinical Epidemiology*. 1994;47(6):671-84.
53. Bohannon RW, DePasquale L. Physical Functioning Scale of the Short-Form (SF) 36: internal consistency and validity with older adults. *Journal of geriatric physical therapy* (2001). 2009;33(1):16-8.
54. Google Maps Platform. Maps Static API: Developer Guide 2019 [cited 2019 July 26]. Available from: <https://developers.google.com/maps/documentation/maps-static/dev-guide>.
55. Barnett AG, McElwee P, Nathan A, Burton NW, Turrell G. Identifying patterns of item missing survey data using latent groups: an observational study. *BMJ open*. 2017;7(10):e017284.
56. Gunn LD, Rozek J, Hooper P, Lowe M, Arundel J, Higgs C, et al. Creating liveable cities in Australia: a scorecard and priority recommendations for Brisbane. 2018.

Tables

Table 1. Characteristics of the HABITAT analytic sample, 2016.

	Low physical function neighbourhood	High physical function neighbourhood
	n=316	n=302
	%	%
Age categories		
45-49	0.95	3.31
50-54	15.19	24.17
55-59	18.99	21.85
60-64	19.62	18.54
65-69	24.68	19.54
70-74	20.57	12.58
Sex		
Male	40.19	45.70
Female	59.81	54.30
Education		
Bachelor+	20.57	56.29
Diploma/Assoc Deg	10.13	8.94
Certificate (trade/Business)	21.84	13.91
None beyond school	47.47	20.86
Occupation		
Mgr/prof	15.54	42.14
White collar	19.26	15.71
Blue collar	14.53	9.29
Home duties	5.74	3.57
Retired	32.77	23.93
Not easily classifiable	12.16	5.36
Household income		
\$130000+	11.18	32.31
\$72800-129999	17.76	22.11
\$52000-72799	9.87	12.59
\$26000-51599	26.97	11.56
Less than \$25999	24.01	6.80
Don't know	3.29	2.72
Don't want to answer	6.91	11.90
Neighbourhood disadvantage		
Q1 (least disadvantaged)	0.00	66.23
Q2	3.16	17.22
Q3	14.87	10.60
Q4	20.57	4.97
Q5 (most disadvantaged)	61.39	0.99

Figures



Figure 1. A customised roadmap image (map type: road map, size: 256x256, zoom level: 19) defined the background as white, roads as black, water as blue, and parks as green.

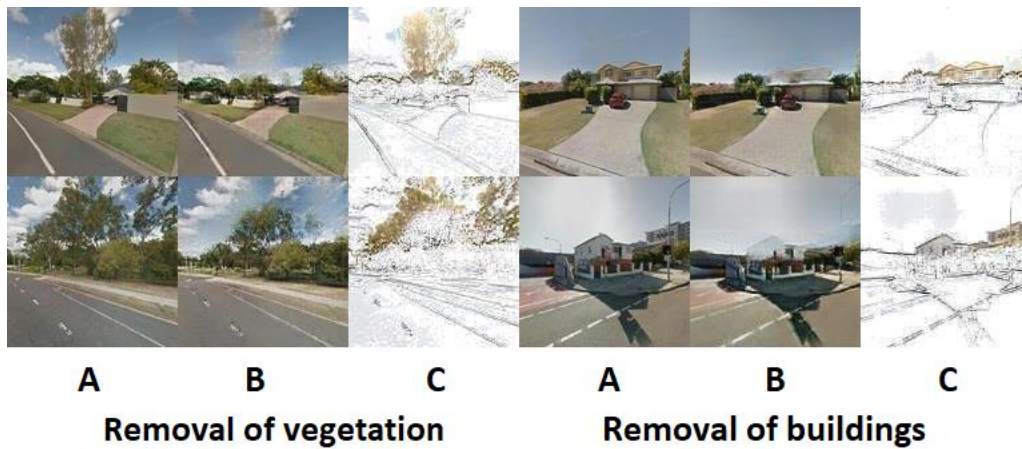
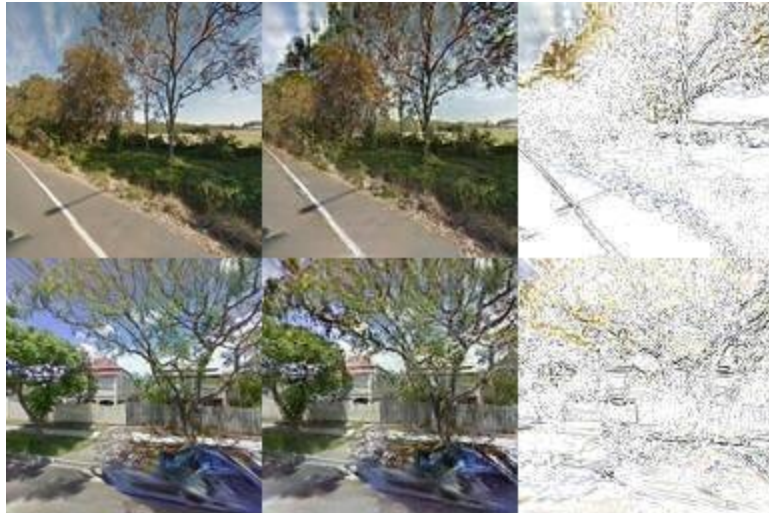


Figure 2. Image translation from 'high physical function' to 'low physical function' neighbourhoods from A) original image, to B) translated image, with C) showing the differences between the two images.



A **B** **C**
Addition of vegetation

Figure 3. Image translation from ‘low physical function’ to ‘high physical function’ neighbourhoods from A) original image, to B) translated image, with C) showing the differences between the two images.